

# FaceSORT: a Multi-Face Tracking Method based on Biometric and Appearance Features

Robert Jöchl and Andreas Uhl

University of Salzburg, Department of Artificial Intelligence and Human Interfaces,  
Salzburg, Austria  
{robert.joechl, andreas.uhl}@plus.ac.at

## Abstract

Tracking multiple faces is a difficult problem, as there may be partially occluded or lateral faces. In multiple face tracking, association is typically based on (biometric) face features. However, the models used to extract these face features usually require frontal face images, which can limit the tracking performance. In this work, a multi-face tracking method inspired by StrongSort, FaceSORT, is proposed. To mitigate the problem of partially occluded or lateral faces, biometric face features are combined with visual appearance features (i.e., generated by a generic object classifier), with both features are extracted from the same face patch. A comprehensive experimental evaluation is performed, including a comparison of different face descriptors, an evaluation of different parameter settings, and the application of a different similarity metric. All experiments are conducted with a new multi-face tracking dataset and a subset of the ChokePoint dataset. The ‘Paris Lodron University Salzburg Faces in a Queue’ dataset consists of a total of seven fully annotated sequences (12730 frames) and is made publicly available as part of this work. Together with this dataset, annotations of 6 sequences from the ChokePoint dataset are also provided.

## 1 Introduction

Multiple object tracking (MOT) [1] is about finding the trajectories of all objects appearing in a sequence. These objects could be from different classes or a single class (e.g. pedestrians, cars, persons, etc.). When considering faces, MOT is referred to as multi-face tracking. This work focuses on tracking the faces of people moving towards a gate in a queue.

The assumed scenario is that a group of people is moving towards a gate (e.g., to enter a sports stadium). As they move towards a single gate, they form a queue. However, as this is a leisure activity, this queue will not be very well organized (people chat with each other, they eat, they move around in a disorderly fashion, there may be pushing and shoving, etc.). In the assumed scenario, the main objective is to track people’s faces as they move towards the gate. For this purpose, a camera is mounted on the gate. The cam-

era is directed at the queue such that the first person visible is standing directly in front of the gate. However, since the queue is probably not very well organized, the main tracking challenges are occlusions (partially and full), out-of-plane rotations (lateral faces) and non-linear motion.

To solve a general MOT problem, basically two paradigms exist: (i) joint-detection-association (JDA), and (ii) tracking-by-detection (TbD). With a JDA based tracker, basically everything is learned (end-to-end), i.e., the object detection, the relevant cues for the association and the association of objects across frames. Recent methods in this context are [2, 3, 4, 5, 6]. In this work, however, the focus is on TbD methods [7, 8, 9, 10, 11, 12]. The first step of a tracker based on the TbD paradigm is the detection of all objects (e.g., faces) in the current frame. The tracking performance is therefore directly related to the detection performance. In [10], a Spatial-Temporal Topology-based Detector (STTD) is proposed. A feature mixing strategy is proposed in [13] to improve the detection performance in the context of MOT. Tracking is then about finding bipartite matches for all detected objects and active tracks (i.e., association problem). A common way to solve this association problem is to apply the Hungarian algorithm [14] to a cost matrix (representing the costs of matching the  $i$ -th active track with the  $j$ -th detected object). These costs can, for example, be based on motion cues and/or appearance cues. Prominent examples for TbD tracker are Simple Online Realtime Tracking (SORT) [15] (motion based association), DeepSORT [16] (associated based on motion and appearance features) and StrongSORT [17] (improved version of DeepSORT). In [12], a transformer is used to estimate complex motion cues. A combination of motion and appearance models in a single network, called UMA, is proposed in [18]. In [9], a fusion of six distance metrics (for motion and appearance cues) is used for association. One advantage of TbD trackers over JDA trackers is that pre-trained models can be utilized for the individual subtasks (e.g., a face detector and face recognition model), while performance is competitive (as demonstrated in [19]). A form of TbD trackers are multi hypothesis trackers [20, 21]. In multi hypothesis tracking, several track hypothesis are maintained simultaneously for the trajectory of each object.

In TbD based multi-face trackers, association is based on (biometric) face features (i.e., deep neural networks trained in the context of face recognition). For example, a two-stage association based on motion and face features (ArcFace [22] trained on the MS-Celeb-1M dataset [23]) is proposed in [24]. Multi-face tracking based on DeepSORT [16] is proposed in [25]. The authors evaluate different combinations of face detectors (i.e. MTCNN [26], SSD [27] and R-FCN [28]) and a face model trained with two different loss functions (i.e., cosine softmax classifier loss [29] and angle softmax classifier loss [30]). Face features of the upper facial regions (i.e. eyes, eyebrows and forehead) are used to track masked faces in [31]. A multi-face tracking method based on SORT [15] (i.e., motion based association) with a similarity matching block (comparing the stored with the currently computed faces features (i.e., ArcFace [22])) as a fallback for all unmatched detections showing a frontal face is proposed in [32]. The method is named ReSORT, because IDs can be recovered based on the similarity matching block. Face features as fallback if motion based association fails is also proposed in [33]. In [34], a single object tracking methods to predict the positions of active tracks (motion cues) is used. The position-based matches are then corrected using face features. A multi-face tracking method based on face features only is presented in [35]. Cumulative learning of face features is performed based on a memory module where selectively redundant features are removed. The proposed method is referred as IdOL (Identity Online Learning). A Multi-Camera Face Detection and Recognition (MCFDR) tracking is proposed in [36]. MCFDR combines YOLO [37] face detection with DeepSORT [16], where SphereFace [38] face features are used for association.

The face features used for tracking are usually based on pre-trained face recognition models (e.g., [22, 39, 40, 41]) that are typically trained on more or less frontal, unoccluded faces. In a multi-face tracking scenario, however, lateral faces (out-of-plane rotations) and partially occluded faces occur. To address this issue, a multi-modality tracker, Online Multi-face Tracking with Multi-modality Cascaded Matching (OMTMCM), is proposed in [42]. The proposed method utilizes body and face features and includes two stages: (i) detection alignment, and (ii) detection association. The detected faces and bodies are aligned in the first stage (i.e., detection alignment). Detection association is performed in a cascade, whereby matching based on face features is performed only with those detections that could not be matched with body features. The face features are extracted by a SeNet [43] pre-trained on the VGGFace2 database [44] and the body features by a ResNet [45] pre-trained on the MovieNet database [46]. However, a corresponding body is not always visible for every detected face, especially in the assumed scenario in which people are moving towards a gate in a queue.

In this work, we propose FaceSORT, a new TbD based multi-face tracker inspired by StrongSORT. Instead of uti-

lizing features extracted from two modalities (e.g., face and body)[42], two different types of features are extracted from the same modality (i.e., detected face). By using two different features from the same image patch, the required presence of body and face, which hardly exists in the considered scenario, is eliminated. The two features (i.e., face features and appearance features) are combined into a single cost value, which forms the basis for association. To the best of our knowledge, FaceSORT is the first multi-face tracking method that combines two features extracted from the same image patch. All other described multi-face trackers [24, 25, 31, 32, 33, 34, 35] rely solely on face features. The combination of the two features helps to better handle lateral or partially occluded faces. FaceSORT is evaluated based on a new multi-face tracking dataset. This dataset reflects the assumed scenario and is released as part of this work. To the best of our knowledge, the published dataset is the first multi-face tracking dataset in which people move in an (unorganized) queue towards a camera (gate). There is only one similar dataset, the ChokePoint dataset [47], in which several people move through a portal. In the released dataset, however, a queue is simulated in which people are talking, eating, pushing, shoving, etc.

In summary, the main contributions of this work are:

- A novel multi-face tracking method (FaceSORT) is proposed that combines two different features (i.e., biometric (face) features and appearance features) extracted from the same image patch.
- A comprehensive experimental evaluation is performed comparing different face feature descriptors, analyzing parameter selection and applying a different similarity metric (i.e., Euclidean distance).
- An ablation study is performed.
- A dedicated multi-face tracking dataset is released. This dataset constitutes of seven annotated sequences (12730 frames) that reflect the assumed scenario (people moving in queue towards a gate).
- Annotations are provided for 6 sequences from the ChokePoint dataset.

The remainder of this paper is organized as follows: the proposed FaceSORT is described in section 2. Section 3 provides an overview of the proposed dataset. The experimental evaluation is described in section 4. An ablation study is conducted in section 5 and the key insights are summarized in the last section 6.

## 2 FaceSORT

FaceSORT is a multi-face tracker based on the basic variant of StrongSORT [17]. Since common face recognition models are usually trained on constrained face images, successful

association (of detected faces and active traces) of lateral or partially occluded faces based on extracted face features can be difficult. To mitigate this problem, FaceSORT combines two different types of features extracted from the same image patch (i.e., detected faces). These features are: (i) face features (representing biometric information), and (ii) appearance features (representing visual appearance). The combination of these features is performed on the cost matrix level.

In common TbD based methods, the association relies on a cost matrix  $C^{n \times m}$ , where  $n$  is the number of active trajectories (tracks) and  $m$  is the number of detected objects. An element  $C_{i,j}$  represents the cost of matching the  $i$ -th active track to the  $j$ -th detected object. The main objective of association is to find bipartite matches where the global cost is minimum (i.e., usually solved by the Hungarian algorithm [14]). In principle,  $C_{i,j}$  is based on a distance  $d$  from a stored/predicted cue of the  $i$ -th active track to a calculated/observed cue of the  $j$ -th detected object and is calculated in FaceSORT as follows,

$$\begin{aligned}
C_{i,j} &= \beta C_{i,j}^{app/bio} + (1 - \beta) C_{i,j}^{pos}, \\
\text{with } C_{i,j}^{app/bio} &= \lambda C_{i,j}^{bio} + (1 - \lambda) C_{i,j}^{app}, \\
\text{and } C_{i,j}^{bio} &= d_{bio}(\Phi_i^{bio}, \Psi_j^{bio}), \\
C_{i,j}^{app} &= d_{app}(\Phi_i^{app}, \Psi_j^{app}), \\
C_{i,j}^{pos} &= d_{pos}(\Phi_i^{pos}, \Psi_j^{pos}).
\end{aligned} \tag{1}$$

The parameter  $\lambda \in \mathbb{R}_{[0,1]}$  weights the contribution of the biometric (face) features ( $C_{i,j}^{bio}$ ) and the appearance features ( $C_{i,j}^{app}$ ). Thus,  $C_{i,j}^{app/bio}$  represents the similarity in terms of biometric cues and visual appearance from a stored face (active track) and a detected face. A spatial distance between a predicted and an observed position is represented by  $C_{i,j}^{pos}$  and weighted by the parameter  $\beta \in \mathbb{R}_{[0,1]}$ .

The set of detected faces at frame  $t$  is denoted by  $\Psi$ , and  $\Psi_j^{bio}$ ,  $\Psi_j^{app}$  and  $\Psi_j^{pos}$  represent the extracted biometric features, the extracted appearance features and the observed position (bounding box), respectively.  $\Phi$  represents the active track memory, storing biometric features  $\Phi^{bio}$ , appearance features  $\Phi^{app}$  and positions  $\Phi^{pos}$  for each active track. A track becomes inactive (is deleted from  $\Phi$ ) if it could not be matched with a detected face in  $N_{max}$  consecutive frames. When a new track is added to  $\Phi$ , it is in a tentative state and is only confirmed if the track could be matched in the next  $N_{init}$  frames. Otherwise, the tentative track is deleted from  $\Phi$ . Similar to StrongSORT, an Exponential Moving Average (EMA) [48] approach is used to update the stored biometric and appearance features from the  $i$ -th matched track, i.e.,

$$\Phi_i^t = \alpha \Phi_i^{t-1} + (1 - \alpha) \Psi_i^t, \tag{2}$$

where  $\Psi_i^t$  represents the extracted features from the current frame  $t$  of the face associated with track  $i$  and the parameter

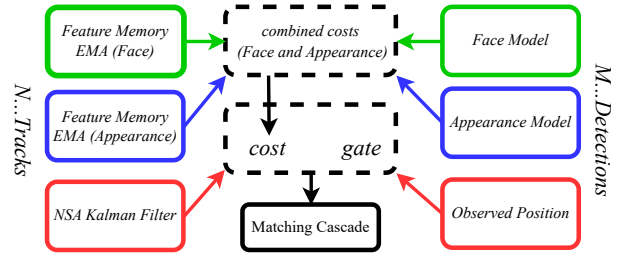


Figure 1: Overview FaceSORT association.

$\alpha$  is a momentum term. As stated in [17], this updating strategy leverages the information of inter-frame feature changes and can mitigate detection noises.  $\Phi$  is maintained separately for biometric and appearance features (i.e.,  $\Phi^{bio}$  and  $\Phi^{app}$ ). The prediction of the position of the  $i$ -th active track ( $\Phi_i^{pos}$ ) in the next frame is based on the NSA Kalman filter [49]. The distance measures used in equation (1) are the cosine similarity ( $d_{bio}$  and  $d_{app}$ ) and the Mahalanobis distance ( $d_{pos}$ ). To avoid uncertain matches,  $C_{i,j}^{app/bio}$  is gated by a maximum spatial distance  $\theta_{pos}$ , i.e.,

$$C_{i,j}^{app/bio} = \begin{cases} \inf & d_{pos}(\Phi_i^{bio}, \Psi_j^{bio}) > \theta_{pos} \\ C_{i,j}^{app/bio} & \text{otherwise} \end{cases}, \tag{3}$$

and a general threshold  $\theta$  is applied, i.e.,

$$C_{i,j} = \begin{cases} \inf & C_{i,j} > \theta \\ C_{i,j} & \text{otherwise} \end{cases}. \tag{4}$$

Based on the cost matrix  $C$ , the bipartite matching problem is formulated as follows,

$$\begin{aligned}
& \text{argmax}_{\alpha_{i,j} \in \{0,1\}} \sum_{i=1}^{|\Phi(t)|} \sum_{j=1}^{|\Psi(t)|} \alpha_{i,j} (C_{max} - C_{i,j}) \\
& \text{s.t. } \begin{cases} \sum_i \alpha_{i,j} \leq 1, & \forall j = 1, \dots, |\Psi(t)| \\ \sum_j \alpha_{i,j} \leq 1, & \forall i = 1, \dots, |\Phi(t)| \end{cases}, \tag{5}
\end{aligned}$$

where  $C_{max}$  denotes the largest element in  $C$  (less than inf). The problem is solved by the Hungarian algorithm [14].

In DeepSORT, a matching cascade is applied in which the matching is performed in sequence, starting with the tracks that were correctly matched in the previous frame and ending with the tracks that have not been matched for the longest time. The matching cascade reduces the search space and could be beneficial when long occlusions are allowed. An overview of the core association procedure of FaceSORT is depicted in Figure 1. For all unmatched detections (after the matching cascade), an IoU-based association (as proposed in SORT [15]) is performed as a fallback routine. The general steps that are performed in FaceSORT for each frame are summarized in Algorithm 1.

## 2.1 Computational Complexity

As shown in Algorithm 1, FaceSORT essentially comprises the matching cascade, the IoU fallback matching, the fea-

---

**Algorithm 1** FaceSORT at frame  $t$ 

---

**Input:**  $\Phi$  and  $\Psi$

- 1: predict position  $\Phi^{pos}$  (Kalman Filter)
- 2:  $\Psi' = \Psi$ ;  $\Phi^+ \subseteq \Phi$  (confirmed tracks)
- 3: **for**  $i = 1, \dots, \max(\Phi^{age})$  **do**
- 4:   **if**  $|\Psi'| > 0$  **then**
- 5:     calculate  $C$  by Eqn. (1) using  $\Phi^{+age=i}$  and  $\Psi'$ ;
- 6:     find matches Eqn. (5)
- 7:     update  $\Psi'$  (unmatched detections)
- 8:   **else**
- 9:     break
- 10:   **end if**
- 11: **end for**
- 12: IoU fallback matching if  $|\Psi'| > 0$
- 13: update/add  $\Phi^{bio}$  and  $\Phi^{app}$  for all detections (Eqn. (2))

---

ture updating and the position prediction. In general, the complexity of finding bipartite matches using the Hungarian algorithm is  $O(|\Phi|^2 \times |\Psi|)$ . This is also the worst case with cascade matching. In the considered scenario, it is very likely that the detected face  $\Psi$  in frame  $t$  were also present in frame  $t - 1$ . Thus, it is reasonable that the complexity can be reduced by the matching cascade (i.e., to  $O((|\Phi|/x)^2 \times \Psi)$ ). For all unmatched detections after the matching cascade, the complexity of the IoU fallback matching is in worst case again  $O(|\Phi|^2 \times |\Psi|)$ . The complexity for updating the memory for biometric and appearance features ( $\Phi^{bio}$  and  $\Phi^{app}$ ) is  $O(|\Psi|)$  in each case. Finally, predicting the positions in frame  $t + 1$  using the Kalman filter has basically a complexity of  $O(\Psi)$ . Thus, the overall complexity of FaceSORT is,

$$O(|\Phi|^2 \times |\Psi| + |\Phi|^2 \times |\Psi| + 2|\Psi| + |\Phi|), \quad (6)$$

which corresponds to the complexity class  $O(|\Phi|^2 \times |\Psi|)$ .

### 3 PLUS Faces in a Queue Dataset

The Paris Lodron University Salzburg Faces in a Queue (PLUSFiaQ) dataset is a new multi-face tracking dataset consisting of a total of seven different sequences. This dataset is made publicly available<sup>1</sup>. An overview of the individual sequences is given in Table 1. In total, the seven sequences comprise 12730 fully annotated frames. This corresponds to about 8 minutes and 30 seconds of video material (25 frames per second). The recorded sequences reflect the assumed scenario (described in section 1), in which several people move towards a gate in a queue. Informed consent was obtained from all participants for all released sequences.

#### 3.1 Scenario Details

The assumed scenario (i.e., queue in front of a gate) is simulated with 12 different people. These persons move towards

Table 1: Sequence (SEQ) details, where F denotes the frames, P the individual person and  $O_d$  the occlusion duration.

SEQ-ID	# F	# P	$\mu(O_d)$	$\sigma(O_d)$	$\min(O_d)$	$\max(O_d)$
01	1774	3	52.00	32.53	29	75
02	3051	12	44.52	55.30	1	500
03	701	12	42.04	50.38	1	250
04	576	10	38.26	38.57	2	206
05	3126	11	39.35	41.88	3	271
06	1301	12	43.68	39.17	4	197
07	2201	10	43.50	45.97	1	257

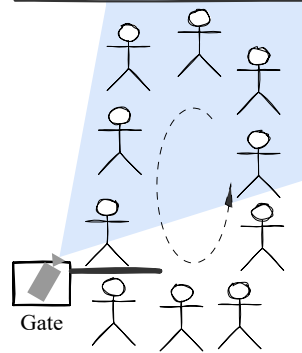


Figure 2: A schematic depiction of the recorded scenario. The area shaded in blue represents the visible area of the camera.

a camera equipped gate. On their way to the gate, they form a queue. However, this queue is not very well organized, i.e., people are chatting, eating, moving quickly, walking backwards, pushing or shoving. As soon as a person has entered the gate, they leave the visible area of the camera and thus the scene. To simulate multiple runs, each person goes more than once through the gate. For this reason, the people move in a counterclockwise circle (as depicted in Figure 2). Thus, when a person re-enters the scene, the person first moves away from the gate (camera). This is also illustrated in Figure 3, where the trajectory of the top-left Bounding-Box coordinates from a specific person is shown (i.e., trID 1702, marked by a red circle). At position (a) the person re-enters the scene, then moves away from the gate (b) until he is roughly farthest away at (c) and then moves towards the gate again at (d) and (e). Finally, the person again leaves the scene (goes through the gate) at position (f). This loop is repeated several times.

The only exception is sequence 1, in which only three people are involved, and they move clockwise, i.e., when they re-enter the scene, they move directly towards the gate. This sequence is also the most simple sequence.

#### 3.2 Annotation Details

Annotations provided comprise a Bounding-Box (BB) for each face, a corresponding tracking identity (trID) and a target class flag. In addition, a visibility measure and a 'next at

<sup>1</sup><https://www.wavelab.at/sources/Joech124b/>



Figure 3: Example of a trajectory of the person with trID 1702.

gate’ flag are included, but these have not been fully adjusted and corrected at this stage. Furthermore, the alignment of the BBs is not defined, thus the contained areas of the face can differ between the BBs.

The trID is a four-digit number (e.g. xxyy), where the first two digits (xx) represent the personal identifiers and the last two digits (yy) represent a consecutive tracking number (per sequence). A new tracking number is assigned when a person has left the scene (goes through the gate) and re-enters the scene again. For example, the person in figure 3 (a), who is directly in front of the gate, has the personal identifier 18. The current tracking number is 1 (i.e., trID 1801). However, after leaving and re-entering the scene, the tracking number is incremented by one (i.e. trID 1802), as shown in Figure 3 (d). For all non-target class objects (faces) a personal identifier of 99 is assigned. The individual non-target class instances are assigned a dedicated tracking number, independent of how often they have re-entered the scene.

For annotation, the VGG Image Annotator (VIA)<sup>2</sup> [50] was used. The corresponding exported annotation file (json file) is provided for each sequence. Furthermore, a Ground-Truth (GT) file according to the MOT20 format [51] is provided additionally, i.e., a csv file where each line represents one object instance and contains 9 values:

*<frame ID>,<trID>,<BB left>,<BB top>,<BB width>,<BB height>,<conf>,<class>,<visibility>*

In case of ground-truth (GT), the 7<sup>th</sup> value (detector confidence score) acts as flag whether the entry is to be considered (i.e., 1: target class, 0: ignore). Since only multiple object (face) tracking is considered, the class label is constantly set to 1. Visibility represents the ratio how much of that object is visible.

As a starting point for the annotation, the BBs detected by yolov5<sup>3</sup> and the trIDs predicted by StrongSORT [17] were used. These BBs and trIDs were then refined manually.

<sup>2</sup><http://www.robots.ox.ac.uk/vgg/software/via>

<sup>3</sup><https://github.com/ultralytics/yolov5>



Figure 4: Examples of tracking challenges.

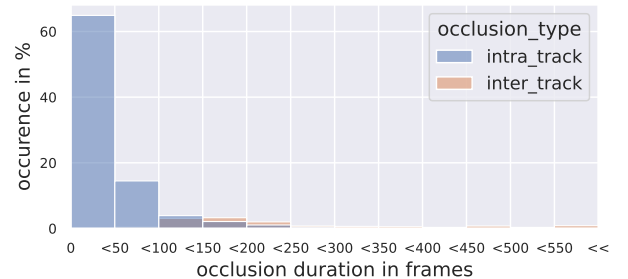


Figure 5: Distribution of occlusion duration. Inter-track occlusions represent the time it takes (in frames) for a person to leave and re-enter the scene.

### 3.3 Tracking Challenges

The PLUSFiaQ dataset comprises various different multi-face tracking challenges. These challenges include: (i) fast motion, (ii) looking down or sideways, (iii) cover the face (e.g., wear a mask), (iv) motion blur (see Figure 4), (v) deformations (i.e., eating or grimacing), (vi) compression artefacts (see Figure 4) and (vi) out-of-plane rotations (see Figure 4). However, the most difficult challenge are likely occlusions.

In Figure 5, the distribution of occlusion duration in frames is illustrated. As can be seen, around 80% of all occlusions are between 1 and 100 frames in length. Inter-track occlu-

sions are those occlusions that occur when a person has left the scene (goes through the gate, the tracking number is incremented by one, e.g., 1801 to 1802), and the inter-track occlusion duration is the time from leaving to re-entering the scene. On average, inter-track occlusions are 257.131 frames long, with maximum occlusion of 1400 frames. The average occlusion duration (intra-track) per sequence as well as minimum and maximum occlusion duration and the standard deviation can be seen in Table 1. In principle, when referring to occlusions, intra-track occlusions are meant. For example, the person with trID 1702 (shown in Figure 3) is occluded 11 times on the way from entering to leaving the scene, with a maximum occlusion duration of 83 frames and a minimum of 3 frames. The average number of occlusions per trID is 0.18, 5.91, 2.42, 3.07, 4.84, 4.89 and 4.03 for sequences 1 to 7, respectively.

## 4 Experimental Evaluation

FaceSORT is evaluated based on the proposed PLUSFiaQ (see section 3) and the ChokePoint[47] dataset. In the ChokePoint dataset, people moving through a portal (chokepoint) are recorded. The dataset comprises sequences from 18 different runs (i.e., different portal, session or walking direction), with 3 different camera perspectives available for each run (i.e.,  $18 \times 3 = 54$  available sequences). Of these 54 sequences, only 6 sequences show multiple persons per frame, which is similar to the assumed scenario in this paper. These 6 sequences are therefore used for evaluation. However, no annotations are available for these 6 sequences and are created accordingly. In the ChokePoint dataset, people are reflected in the open glass door as they walk through the portal. These reflections are annotated as non-target classes. The annotations created have the same format as described in section 3 and are made available along with the PLUSFiaQ dataset.

### 4.1 Tracker Implementation

FaceSORT is implemented based on the StrongSORT implementation<sup>4</sup>. The parameter  $\alpha$  for the EMA feature updating strategy is set to  $\alpha = 0.9$ . The weighting parameter  $\beta$  (for weighting the contribution of biometric and appearance similarity compared to spatial distance) is set to 0.98. This gives the biometric and appearance similarity the most weight.  $\theta_{pos}$  is set to 9.4877 (the 0.95 quantile of the chi-squared distribution with 4 degrees of freedom). These parameters are set according to [17]. The general cost threshold  $\theta$  is set to 0.2 and the minimum IoU (fallback routine) to 0.3. For all experiments,  $N_{init} = 1$  and the maximum age parameter is set to  $N_{max} = 100$  frames (i.e., all tracks that were not successfully matched for more than 100 frames are deleted). With this setting, most occlusions are taken into account while avoiding interference from inter-track oc-

sions (as shown in Figure 5). As face detector yolov8<sup>5</sup> with a confidence score threshold of 0.4 is used.

### 4.2 Evaluated Features

To extract the appearance features, a generic object classification model is used, i.e., a ResNet [45] trained on the ImageNet dataset [52] (resnet18 imported from torchvision models). The appearance features are combined with several different face (biometric) features. The python framework DeepFace [53, 54] provides a wrapper for multiple state-of-the-art face descriptors, i.e., VGG-Face based on the VGG-Very-Deep-16 CNN architecture [39] and evaluated on the Faces in the Wild [55] and the YouTube Faces [56] dataset, Facenet [40] trained on the CASIA-WebFace [57] and the VGGFace2 [44] database, OpenFace [58] trained on the CASIA-WebFace [57] and FaceScrub [59] dataset (based on paper), DeepFace [60] trained on a large collection of Facebook images (i.e., the Social Face Classification (SFC) dataset), DeepID [61] trained on the Faces in the Wild [55] dataset and tested, ArcFace [22, 62], SFace [41] trained on CASIA-WebFace [57] VGGFace2 [44] and MS1MV2 and Dlib [63] trained on the VGG-Face [39] and FaceScrub [59] dataset (plus a large number of images the author scraped from the internet). All these different face descriptors provided by DeepFace are evaluated. DeepFace also provides a 512 dimensional face descriptor for Facenet (i.e., Facenet512) and ArcFace (ArcFaceII) is also evaluated based on a different implementation<sup>6</sup>. In addition, the face descriptor used in [42], SeNet [43], is evaluated.

### 4.3 Evaluation Metrics

The Multiple Object Tracking Accuracy (MOTA)[64] is a commonly used metric for evaluating multiple object tracking methods. With MOTA, tracking errors are accumulated on a frame-by-frame basis, i.e., wrongly detected objects (False Positive (FP)), missed objects (False Negative (FN)) and identity switches (IDSWs) are counted for each frame ( $t$ ), summed up and normalized by the total amount of objects in the ground-truth (GT),

$$MOTA = 1 - \frac{\sum_t (FP_t + FN_t + IDSW_t)}{|GT|}. \quad (7)$$

An IDSW occurs if the ID assigned in the previous frame ( $t-1$ ) differs from the ID assigned in the current frame ( $t$ ). As MOTA only considers the previous frame, the entire tracking performance of an object during its lifetime is not taken into account. For example, if an object is tracked correctly for 90% of its lifetime but yields the same number of IDSW as an object that is only tracked correctly for 60%, the same MOTA score is achieved. Furthermore, the MOTA score can be dominated by the detector performance (i.e., TP and FP).

<sup>4</sup><https://github.com/dyhBUPT/StrongSORT>

<sup>5</sup><https://github.com/ultralytics/ultralytics>

<sup>6</sup><https://github.com/mobilesec/arcface-tensorflowlite>

Since the face detection is fixed for all experiments, only the normalized IDSW is calculated, i.e.,

$$IDSW = \frac{\sum_t IDSW_t}{|GT|}. \quad (8)$$

A metric that focuses on the entire sequence (how long an object is correctly tracked) is the IDF1 [65], i.e.,

$$IDF1 = \frac{2IDTP}{2IDTP + IDFP + IDFN}, \quad (9)$$

where IDTP are the correct tracked objects, IDFP are tracked objects that do not match any ground-truth object and IDFN are objects in the ground-truth that are not tracked. The global assignment of tracker hypothesis and ground-truth objects is performed using the suggested truth-to-result match procedure, i.e. the combination that yields the highest IDF1 score is selected.

The Higher Order Tracking Accuracy (HOTA)[66],

$$HOTA_\alpha = \sqrt{DetA_\alpha \cdot AssA_\alpha}, \quad (10)$$

is an evaluation metric for assessing MOT trackers, where  $DetA_\alpha$  and  $AssA_\alpha$  denote the detection and association accuracy at localization threshold  $\alpha$ . The localization threshold represents the minimum IoU that a detected BB and a ground-truth BB must reach in order to consider the corresponding ground-truth object as detected (i.e. as TP detection). Thus, HOTA combines all three different aspects for MOT tracker evaluation (i.e., localization, detection and association performance) into a single score. To evaluate the different components individually, HOTA can be decomposed into submetrics. In the considered experimental evaluation, only the association performance is relevant (the detected BBs and locations are fixed for all experiments).

To measure the association performance, the authors in [66] propose the concept of True Positive Associations (TPAs), False Negative Associations (FNAs) and False Positive Associations (FPAs). TPAs are the set of all correctly tracked TPs (correctly detected objects), while FNAs are the set of TPs that are assigned different trIDs for the same ground truth ID (gtID), and FNAs (not detected objects). In other words, FNAs represent the amount of intra-person trID switches. On the contrary, FPAs are the set of TPs with the same trID but different gtIDs (i.e., inter-person trID switches), and FPAs (wrongly detected objects). Based on the TPAs, FNAs and FPAs the association recall (AssRe), i.e.,

$$AssRe_\alpha = \frac{1}{|TP|} \sum_{c \in \{TP\}} \frac{|TPA(c)|}{|TPA(c)| + |FNA(c)|}, \quad (11)$$

and association precision (AssPr), i.e.,

$$AssPr_\alpha = \frac{1}{|TP|} \sum_{c \in \{TP\}} \frac{|TPA(c)|}{|TPA(c)| + |FPA(c)|}, \quad (12)$$

can be computed. A combination (Jaccard index) of AssRe and AssPr is the association accuracy (AssA), i.e.,

$$AssA_\alpha = \frac{AssRe_\alpha \cdot AssPr_\alpha}{AssRe_\alpha + AssPr_\alpha - AssRe_\alpha \cdot AssPr_\alpha}. \quad (13)$$

In HOTA, AssA is the main measure for association performance. For all reported results,  $\alpha = 0.2$ .

## 4.4 Experimental Results

In FaceSORT, the selection of the weighting parameter  $\lambda$  (combination of biometric and appearance features) and the association threshold  $\theta$  is crucial. Thus, the parameter selection is evaluated in detail along with different face features and a different similarity metric (Euclidean distance instead of cosine similarity).

### 4.4.1 Selection of a fixed $\lambda$

Table 2: PLUSFiaQ: maximum AssA and IDF1 as well as minimum IDSW, with the corresponding  $\lambda$  selection.

	$\lambda$	AssA $\uparrow$	$\lambda$	IDF1 $\uparrow$	$\lambda$	IDSW $\downarrow$
ArcFace	0.1	0.6461	0.1	0.7342	0.0	0.0088
DeepFace	0.1	0.6494	0.1	0.7411	0.0	0.0088
DeepID	0.0	0.6303	0.0	0.7277	0.2	0.0083
Dlib	0.0	0.6303	0.0	0.7277	<b>0.4</b>	<b>0.0082</b>
Facenet	0.1	0.6355	0.1	0.7308	0.0	0.0088
Facenet512	<b>0.1</b>	<b>0.6550</b>	0.1	0.7397	0.0	0.0088
OpenFace	0.1	0.6547	<b>0.1</b>	<b>0.7466</b>	0.0	0.0088
SFace	0.1	0.6527	0.1	0.7338	0.0	0.0088
SeNet50	0.2	0.6425	0.2	0.7396	0.2	0.0084
VGG-Face	0.1	0.6515	0.1	0.7405	0.0	0.0088
ArcFaceII	0.1	0.6451	0.1	0.7333	0.0	0.0088

Table 3: ChokePoint: maximum AssA and IDF1 as well as minimum IDSW, with the corresponding  $\lambda$  selection.

	$\lambda$	AssA $\uparrow$	$\lambda$	IDF1 $\uparrow$	$\lambda$	IDSW $\downarrow$
ArcFace	0.2	0.8364	0.1	0.8754	0.3	0.0068
DeepFace	0.6	0.8359	0.3	0.8755	0.0	0.0076
DeepID	0.6	0.8306	0.2	0.8756	0.0	0.0076
Dlib	0.5	0.8353	0.1	0.8752	<b>1.0</b>	<b>0.0052</b>
Facenet	0.3	0.8306	0.0	0.8724	0.0	0.0076
Facenet512	0.1	0.8355	0.1	0.8773	0.1	0.0075
OpenFace	0.2	0.8298	0.2	0.8728	0.0	0.0076
SFace	0.1	0.8404	0.1	0.8783	0.0	0.0076
SeNet50	0.4	0.8325	0.4	0.8740	0.5	0.0069
VGG-Face	<b>0.3</b>	<b>0.8497</b>	<b>0.2</b>	<b>0.8819</b>	0.0	0.0076
ArcFaceII	0.2	0.8396	0.1	0.8777	0.0	0.0076

Figure 6 shows the average (across all sequences) AssA and IDF1 scores as well as the normalized amount of IDSW for all evaluated face descriptors and different  $\lambda$  selections. In general, the higher the AssA or IDF1 score or the lower the number of IDSWs, the better the tracking performance. The scores achieved when setting  $\lambda$  to 1.0 can be considered as the baseline. In this setting, only face (biometric) features are taken into account (essentially corresponds to StrongSORT with matching cascade). When looking at AssA and IDF1,

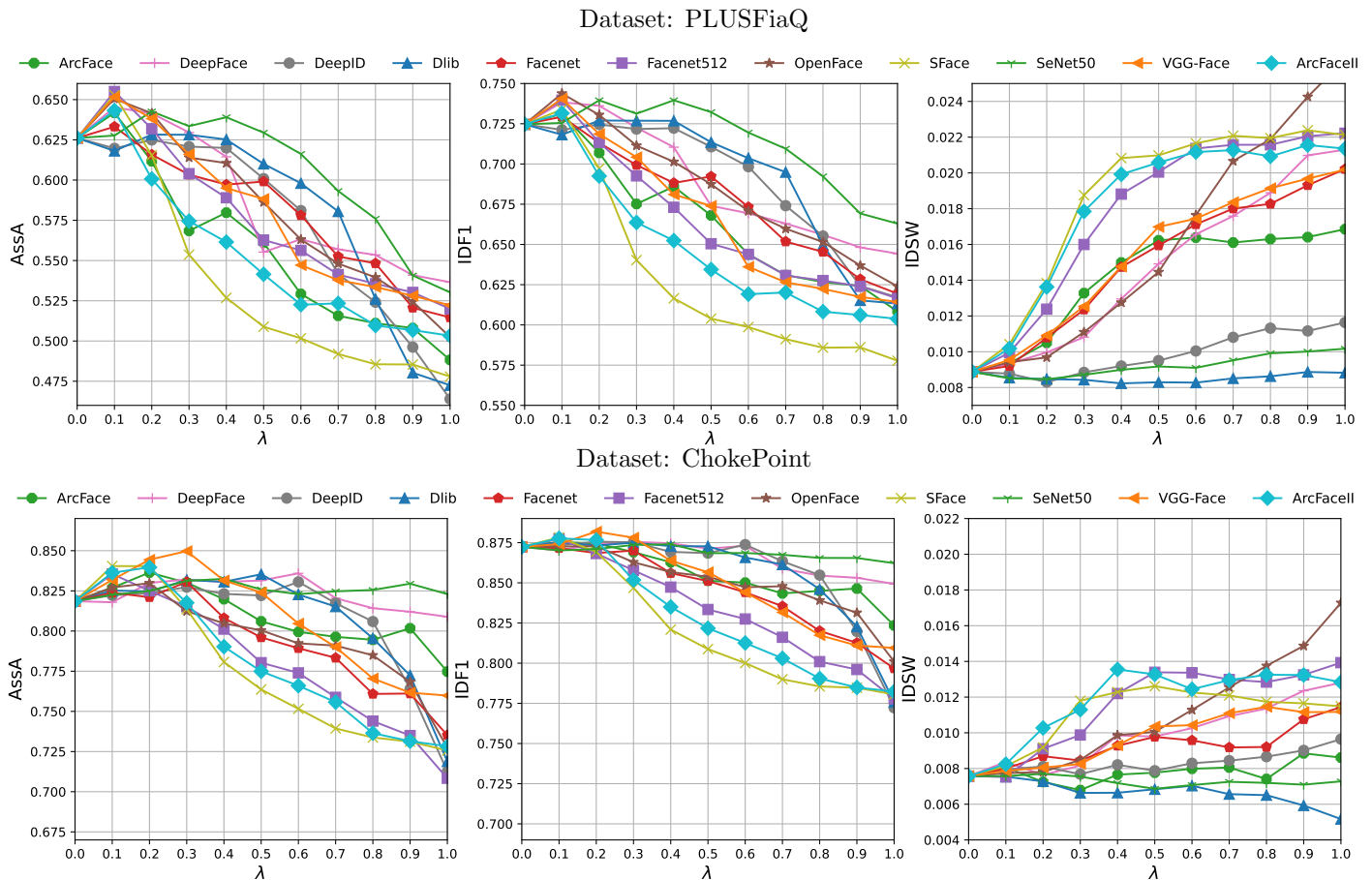


Figure 6: The average (across all sequences) AssA and IDF1 scores as well as the normalized amount of IDSW for all evaluated face descriptors and  $\lambda$  selections. Recall: for AssA and IDF1, the higher the better, and for IDSW, the lower the better.

a general increase in scores can be observed with increasing influence of the appearance feature (i.e.  $\lambda \rightarrow 0$ ). The number of IDSWs, on the other hand, decreases. Thus, the tracking performance increases when  $\lambda$  decreases (i.e., with increasing influence of the appearance feature).

The best values achieved (i.e. max. AssA and IDF1 as well as min. IDSW) are shown together with the corresponding  $\lambda$  values in tables 2 and 3. In general, significantly higher results are achieved with the ChokePoint dataset (i.e., the PLUSFiaQ dataset is more challenging). With the PLUSFiaQ dataset, the best results (AssA and IDF1) are achieved at  $\lambda = 0.1$  (except for Dlib, DeepID and SeNet50). In contrast, the best results are achieved with the Chokepoint dataset having  $\lambda$  values up to 0.6. One reason for this could be that with the ChokePoint dataset, people look towards the camera when they approach the portal, which facilitates biometric features. The number of IDSWs is usually lowest at  $\lambda = 0.0$  (i.e., when only appearance features are used). However, it can be stated that the combination of biometric and appearance features improves tracking performance.

In multi-face tracking, inter-person trID switches (i.e.,

when the trID is switched to an existing trID of a different person) are likely to be more critical than intra-person trID switches (i.e., when a new trID is assigned). As already described, the AssPr score reflects the FPAs (i.e., inter-person trID switches) and is illustrated in Figure 7. If only face (biometric) features are used for association (i.e.  $\lambda = 1.0$ ), inter-person identity switches are expected to be limited, as the extracted face (biometric) features should be distinct for different persons. For both analyzed datasets, this can basically be observed for 4/11 evaluated face descriptors (i.e., SFace, ArcFaceII, VGG-Face and Facenet512), with SFace showing the most consistent and best results. However, the AssPr decreases as  $\lambda$  decreases. This is reasonable as the association in reducing  $\lambda$  is more and more based on generic appearance features and the appearance of two different faces may be similar, while the face (biometric) features are distinct. Considering that the best AssA for these 4 face descriptors is reached at lower  $\lambda$  values (i.e., 0.1-0.3 for the ChokePoint and 0.1 for the PLUSFiaQ dataset), the higher AssA is accompanied by a decrease in AssPr (i.e., an increase in inter-person trID switches (FPAs)). In contrast, the AssPr



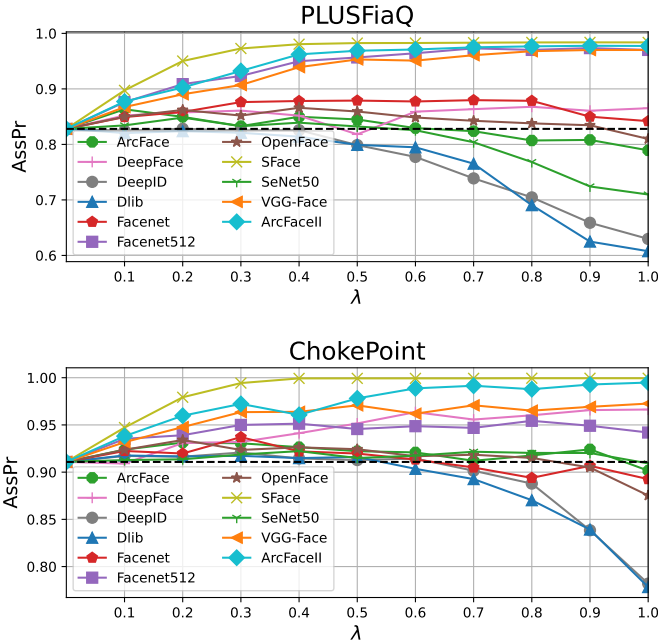


Figure 7: Average AssPr (across all evaluated sequences).

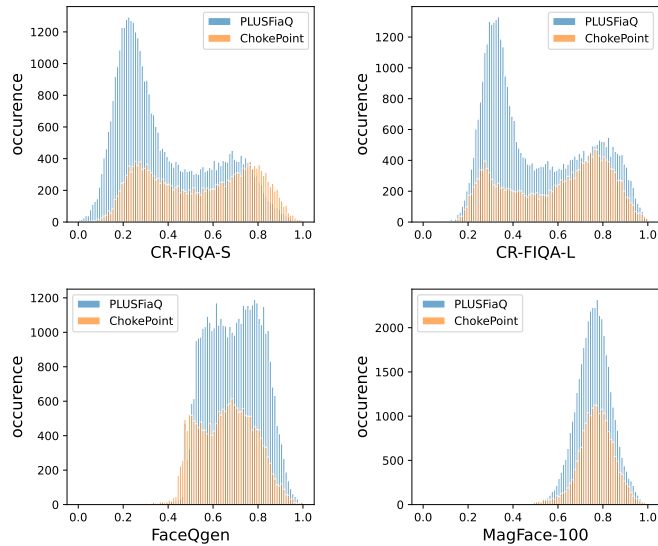


Figure 8: Quality score distribution.

for Dlib and DeepID is much lower for  $\lambda = 1.0$  than compared to the generic feature baseline (Figure 7 dotted black line). This would indicate weak face descriptors for the considered evaluated sequences.

#### 4.4.2 Selection of a dynamic $\lambda$ based on Face Quality

By setting the parameter  $\lambda$  to a fixed value (e.g.  $\lambda = 0.1$ ), the weighting between biometric and optical features is constant for each image and each detected face, regardless of the

biometric information present in the extracted face patch. For this reason, a more natural approach would be for  $\lambda$  to reflect the available biometric information (i.e.,  $\lambda = 1$  when full biometric information is available and  $\lambda = 0$  when no biometric information is available). The biometric information present in a face sample can be quantified by a face quality score [67, 68, 69]. For this reason, another option would be to set  $\lambda$  dynamically according on a face quality score. This turns  $\lambda$  into an  $m \times n$  matrix with constant columns corresponding to the face quality scores of the  $n$  detected faces. The multiplications  $\lambda C_{bio}$  and  $(1 - \lambda)C_{app}$  are then element wise multiplications.

Three different face quality models are exploited, i.e., CR-FIQA [67], MagFace [68] and FaceQgen [69]. In case of the CR-FIQA two different backbone model sizes are evaluated, i.e., CR-FIQA-S and CR-FIQA-L. To obtain a face quality score the detected face patch is fed into the respective model. The distribution of quality scores achieved for all detected faces (across all sequences) is illustrated in Figure 8. Quality values that are not restricted to  $\mathbb{R}_{[0,1]}$  are normalized by dividing by the maximum observed value.

In Figure 9, the results are compared between a fixed (best results table 2 and 3) and a dynamically set (based on face quality scores)  $\lambda$ . It can be seen that tracking performance is generally lower when  $\lambda$  is dynamically set based on face quality scores. Only with CR-FIQA is the performance for some face descriptors as high as when  $\lambda$  is set to a fixed value. In general, the performance based on CR-FIQA is consistently better than the other two face quality models evaluated. The better performance of CR-FIQA could be expected when looking at the distribution of face quality scores (Figure 8), as FaceQgen and MagFace only cover a limited range, while CR-FIQA covers almost the entire range from 0 to 1, which appears more natural. Thus, the reasonable approach of dynamically setting  $\lambda$  based on available biometric information (face quality scores) is not working. A reason for this could be that the considered face quality scores do not reflect the actual biometric information present.

#### 4.4.3 Grid Search

To assess whether a higher AssA can be achieved with a dynamic  $\lambda$  (which is different for each detected face) than with a fixed  $\lambda$ , a grid search is performed. In a grid search, all possible combinations of  $\lambda$  are evaluated. For example, if 5 faces are detected per frame and 11 different  $\lambda$  values are allowed (i.e.  $\lambda \in [0.0, 0.1, 0.2, 0.3, 0.4, 0.5, 0.6, 0.7, 0.8, 0.9, 1.0]$ ), this would result in  $11^5$  different combinations for the frame under consideration. Since the association in the current frame depends on the past frames, the different combinations must be considered across all frames, i.e.  $\prod_{i=1}^N 11^{m^i}$  combinations, where  $N$  is the number of frames and  $m^i$  are the detected faces for the  $i$ -th frame. This is simply not computable. Thus, only a local grid search (between two consecutive frames) is performed. More precisely, the AssA

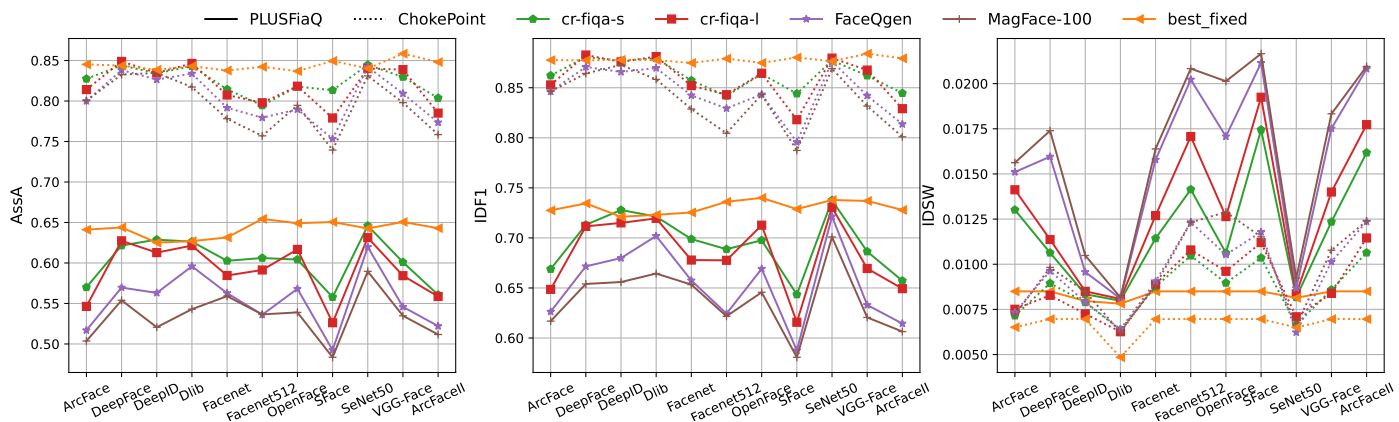
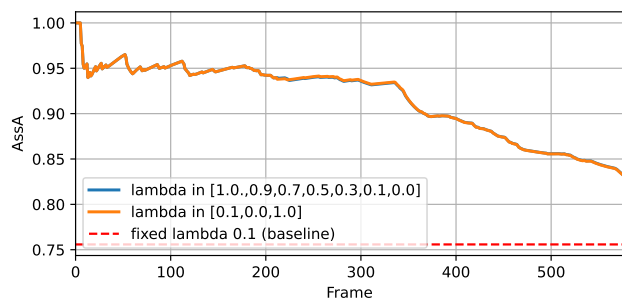
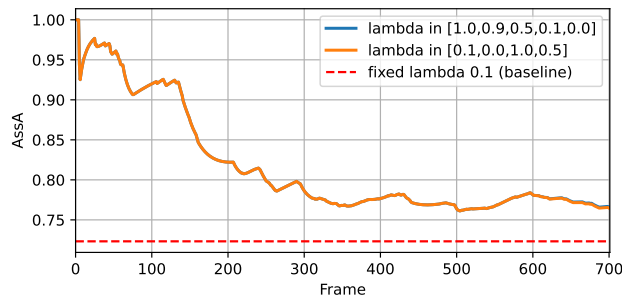


Figure 9: Achieved AssA, IDF1 and IDSW with  $\lambda$  dynamically set based on normalized (by the maximum value) face quality values compared to the best achieved AssA, IDF1 and IDSW based on a fixed  $\lambda$  value. Recall: for AssA and IDF1, the higher the better, and for IDSW, the lower the better.



(a) sequence ID 04

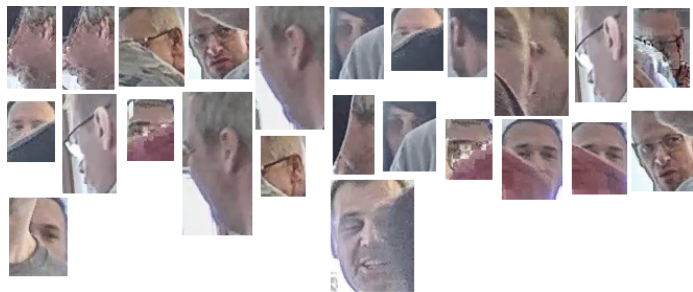


(b) sequence ID 03

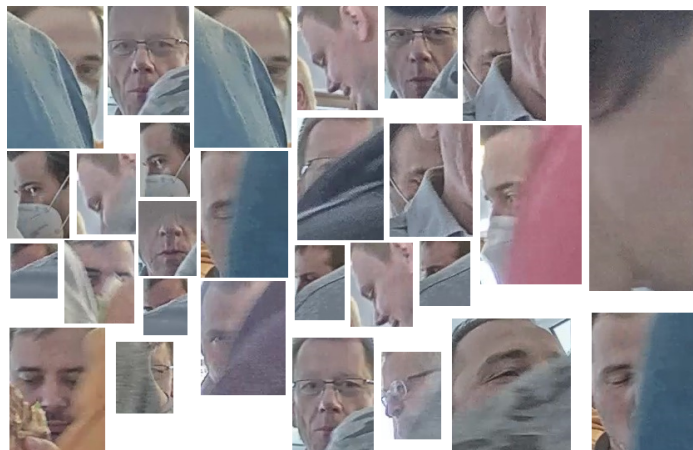
Figure 10: Highest AssA achieved per frame in the grid search.

is calculated after each  $\lambda$  combination for the current frame. The combination that achieves the highest AssA is selected. If several combinations achieve the highest AssA, the combination that achieves the highest AssA first is selected.

Since the evaluation of 11 different  $\lambda$  values is still very time-consuming, a smaller number is considered. In addition, the grid search is only performed with the best face descriptor (in terms of AssPr), SFace, and only for the two sequences



(a) sequence ID 04



(b) sequence ID 03

Figure 11: Face patches that were assigned a  $\lambda$  of 1.0 during the grid search.

with the fewest frames (sequence ID 3 and 4). In Figure 10 (a), the highest AssA achieved for each frame of sequence 4 is illustrated. It can be seen that the AssA at frame 576 (complete sequence) is about 0.09 higher than the baseline (fixed  $\lambda$ ) and exactly the same results are obtained regardless

of whether  $\lambda$  is selected from [1.0,0.9,0.7,0.5,0.3,0.1,0.0] or [1.0,0.1,0.0].

Taking into account possible  $\lambda$  values of [1.0,0.9,0.7,0.5,0.3,0.1,0.0], a  $\lambda$  of 1.0 is selected for 2199/2239 detected faces in sequence 04. The  $\lambda$  values for the remaining 40 detected faces are distributed as follows: 5, 22, 7, 4, 2 for the  $\lambda$  values 0.0, 0.1, 0.3, 0.5 and 0.7, respectively. The vast majority of  $\lambda$  values are set to 1.0 because the grid search conducted always selects the first  $\lambda$  combination that achieves the highest AssA value, and the first combination tried is that all  $\lambda$  values equal 1.0. In the version where  $\lambda$  can be chosen from only three values (i.e. [0.1,0.0,1.0]), the first combination tried is that all  $\lambda$  values are equal to 0.1, and the last combination is that all  $\lambda$  values are equal to 1.0 (i.e. a  $\lambda$  of 1.0 is only chosen if 0.1 and 0.0 do not achieve an equally high AssA). In this case, a  $\lambda$  of 0.1 is selected for 2206/2239 detected faces. Compared to the baseline (i.e. fixed  $\lambda$  of 0.1 for all recognized faces), a change of  $\lambda$  for only 33 recognized faces yields the performance gain. In particular, for 24 detected faces, a  $\lambda$  value of 1.0 is selected. A  $\lambda$  value of 1.0 means that only face features are used. Therefore, it is expected that the corresponding face patches contain adequate biometric information. The 24 face patches where  $\lambda$  is set to 1.0 are illustrated in Figure 11 (a). As can be seen, the biometric information is very limited.

The results for sequence 3 are similar. In Figure 10 (b), the highest AssA achieved for each frame is illustrated. If the possible  $\lambda$  values are [0.1, 0.0, 1.0, 0.5], a value of 0.1 is selected for 2431/2466 detected faces. A  $\lambda$  value of 0.0, 0.5 and 1.0 is selected for 6, 1 and 28 recognized faces, respectively. Again, it would be expected that with a selected  $\lambda$  value of 1.0, there should be reasonable biometric information in the face patches. However, as can be seen in Figure 11 (b) the biometric information in all 28 face patches is limited.

These observations indicate that linking  $\lambda$  to the available biometric information does not lead to better performance.

#### 4.4.4 Matching Score Distribution

A multi-face tracker can be compared with a biometric system (e.g., a set of query images (detected faces) are matched against a database of enrolled identities (active tracks)). Matching is based on a similarity score, and in a perfect system, the genuine scores do not overlap with the imposter scores. In the context of FaceSORT, the genuine scores represent the cosine similarity that result when a detected face is compared with the corresponding stored faces (active tracks). The imposter scores, on the other hand, represent the cosine similarities that are achieved when a detected face is compared with all other stored faces (tracks). Table 4 shows the mean and the standard deviation of the genuine and the imposter score distribution as well as their overlap (IoU). Considering the IoU, the most distinct face descriptor (lowest IoU) is SFace. Other face descriptors with a low IoU

Table 4: Presents the overlap (IoU) between the genuine and imposter scores as well as their mean ( $\mu$ ) and standard deviation ( $\sigma$ ). Feature models: (1) ArcFace, (2) DeepFace, (3) DeepID, (4) Dlib, (5) Facenet, (6) Facenet512, (7) OpenFace, (8) SFace, (9) SeNet50, (10) VGG-Face, (11) ArcFaceII and (12) Appearance Features.

	PLUSFiaQ			ChokePoint		
	IoU	genuine $\mu/\sigma$	imposter $\mu/\sigma$	IoU	genuine $\mu/\sigma$	imposter $\mu/\sigma$
(1)	0.26	0.14/0.14	0.52/0.31	0.20	0.15/0.14	0.57/0.29
(2)	0.14	0.10/0.07	0.25/0.08	0.12	0.10/0.08	0.26/0.08
(3)	0.20	0.02/0.03	0.09/0.06	0.17	0.03/0.04	0.10/0.06
(4)	0.07	0.02/0.01	0.07/0.02	0.08	0.02/0.01	0.08/0.03
(5)	0.18	0.12/0.12	0.51/0.25	0.26	0.13/0.13	0.46/0.27
(6)	0.07	0.16/0.14	0.76/0.20	0.09	0.19/0.15	0.73/0.22
(7)	0.18	0.10/0.08	0.31/0.14	0.18	0.11/0.09	0.35/0.17
(8)	<b>0.04</b>	0.27/0.17	0.87/0.13	<b>0.04</b>	0.29/0.17	0.90/0.12
(9)	0.18	0.02/0.03	0.09/0.06	0.19	0.05/0.07	0.25/0.16
(10)	0.07	0.15/0.11	0.60/0.15	0.08	0.20/0.12	0.67/0.17
(11)	0.08	0.21/0.15	0.77/0.18	0.05	0.23/0.14	0.82/0.16
(12)	0.16	0.03/0.03	0.28/0.19	0.18	0.03/0.04	0.26/0.18

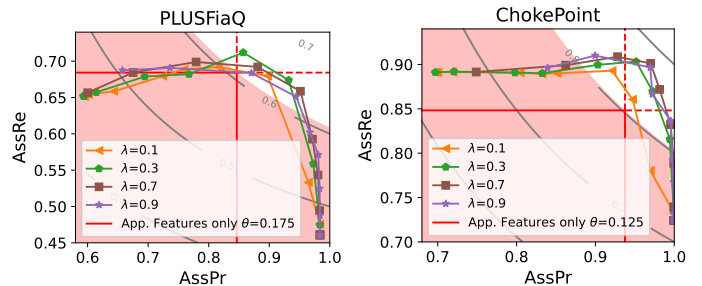


Figure 12: AssRe over AssPr for different  $\theta$  and  $\lambda$  combinations and SFace features. The  $\theta$  values increase from left to right and the contour lines represent the AssA, where the area shaded in red indicates a lower AssA than for the best achieved AssA when only appearance features are used.

are Facenet512, VGG-Face, ArcFaceII and Dlib. These face descriptors (except Dlib) are also the face descriptors achieving the highest AssPr (see Figure 7). However, based on the IoU results, it is surprising that such low AssPr values are obtained with the Dlib face descriptor. A reason for the low AssPr values could be that, with a mean value of 0.07, the imposter scores are well below the threshold  $\theta = 0.2$  (applied to reject uncertain (imposter) matches). Thus, a closer look is taken at the selection of the threshold value  $\theta$ .

#### 4.4.5 Selection of the Threshold $\theta$

For both datasets, the genuine and imposter scores obtained on the basis of the Dlib features are close to zero (see Table 4). Thus, with a threshold  $\theta = 0.2$  possible imposter matches (inter-person identity switches) are not rejected. This explains the low AssPr value when only Dlib features are used for the association ( $\lambda = 1.0$ ), although the genuine and imposter distributions are relatively distinct (an IoU value of 0.07 and 0.08). If  $\theta$  is set to 0.025, an AssPr of 0.9831

Table 5: Best achieved AssA, IDF1 and IDSW for different selections of  $\theta$  and  $\lambda$  combinations. Face descriptors: (1) ArcFace, (2) DeepFace, (3) DeepID, (4) Dlib, (5) Facenet, (6) Facenet512, (7) OpenFace, (8) SFace, (9) SeNet50, (10) VGG-Face and (11) ArcFaceII.

	PLUSFiaQ						ChokePoint					
	$\theta/\lambda$	AssA $\uparrow$	$\theta/\lambda$	IDF1 $\uparrow$	$\theta/\lambda$	IDSW $\downarrow$	$\theta/\lambda$	AssA $\uparrow$	$\theta/\lambda$	IDF1 $\uparrow$	$\theta/\lambda$	IDSW $\downarrow$
(1)	0.2/0.1	0.6461	0.2/0.1	0.7342	0.35/0.1	0.0080	0.2/0.2	0.8364	0.2/0.1	0.8754	0.56/0.1	0.0054
(2)	0.2/0.1	0.6494	0.2/0.1	0.7411	0.3/0.1	0.0078	0.25/0.4	0.8446	0.25/0.4	0.8840	0.3/0.2	0.0053
(3)	0.175/0.1	0.6399	0.175/0.1	0.7349	0.2/0.2	0.0083	0.15/0.4	0.8376	0.15/0.4	0.8778	0.2/0.0	0.0076
(4)	0.175/0.0	0.6373	0.175/0.0	0.7287	0.2/0.4	0.0082	0.2/0.5	0.8353	0.2/0.1	0.8752	0.2/1.0	0.0052
(5)	0.175/0.0	0.6373	0.21/0.1	0.7337	0.35/0.1	0.0079	0.21/0.1	0.8314	0.21/0.1	0.8759	0.56/0.5	0.0051
(6)	<b>0.3/0.3</b>	<b>0.6693</b>	0.3/0.3	0.7520	0.4/0.2	0.0078	0.3/0.3	0.8493	0.4/0.4	0.8812	0.7/0.2	0.0049
(7)	0.25/0.3	0.6589	0.25/0.3	0.7505	0.3/0.2	0.0077	0.2/0.2	0.8298	0.2/0.2	0.8728	0.35/0.4	0.0052
(8)	0.4/0.4	0.6663	<b>0.4/0.3</b>	<b>0.7559</b>	<b>0.6/0.5</b>	<b>0.0072</b>	<b>0.5/0.5</b>	<b>0.8879</b>	<b>0.5/0.5</b>	<b>0.9075</b>	<b>0.8/0.2</b>	<b>0.0046</b>
(9)	0.2/0.2	0.6425	0.2/0.2	0.7396	0.25/0.3	0.0077	0.25/0.7	0.8457	0.25/0.3	0.8811	0.35/0.6	0.0050
(10)	0.2/0.1	0.6515	0.2/0.1	0.7405	0.3/0.1	0.0079	0.3/0.6	0.8581	0.3/0.6	0.8875	0.8/0.8	0.0048
(11)	0.3/0.2	0.6572	0.3/0.2	0.7433	0.4/0.2	0.0078	0.4/0.5	0.8611	0.4/0.5	0.8928	0.6/0.6	0.0047
$\emptyset$	0.23/0.16	0.6505	0.24/0.16	0.7413	0.33/0.22	0.0078	0.27/0.40	0.8470	0.28/0.33	0.8828	0.49/0.42	0.0053

and 0.9938 is achieved for the PLUSFiaQ and ChokePoint datasets respectively. This shows that, in addition to  $\lambda$ ,  $\theta$  is an important parameter as well. In Table 5, the best achieved AssA, IDF1 and IDSW values for different  $\theta$  and  $\lambda$  combinations are shown. It can be seen that the initial choice of  $\theta = 0.2$  was already pretty good for several face descriptors. Overall, the best results are achieved with SFace, which also provides the most distinctive, genuine and imposter score distributions (IoU of 0.04). Again, the  $\lambda$  values with which the best results are achieved are significantly higher for the ChokePoint dataset (probably less occlusions and lateral faces benefit biometric features). Although very low  $\theta$  values (e.g. 0.0125, 0.025, 0.05, etc.) were evaluated, no combination of Dlib and appearance features achieved higher tracking performance than with appearance feature only (i.e.  $\lambda = 0.0$ ).

When considering the threshold  $\theta$  the expectation is that the AssPr is very high for low  $\theta$  values (reject most imposter matches) and it decreases when  $\theta$  increases. However, a low value of  $\theta$  can lead to a lower AssRe (more intra-person trID switches) since also genuine matches are rejected. In Figure 12 the trade-off between AssRe and AssPr compared to AssA (contour lines) for the best face descriptor SFace is shown for different  $\lambda$  and  $\theta$  combinations. The  $\theta$  values decrease from left to right (i.e., 0.9, 0.8, 0.7, 0.6, 0.5, 0.4, 0.3, 0.2, 0.1, 0.05 and 0.025) and the red lines show the AssRe and AssPr for the best AssA achieved with appearance features only (baseline). The area shaded in red represents the area where the AssA is lower than the baseline. A good trade-off (relatively constant high AssPr while reducing intra-person IDSWs (AssRe)) when increasing the threshold  $\theta$  can be achieved for higher  $\lambda$  values (higher contribution of biometric features).

#### 4.4.6 Selection of the Similarity Metric

Another factor that can influence the tracking performance is the selection of the similarity metric (used to compute  $C_{i,j}^{app/bio}$ ). The best results achieved when using Euclidean distance instead of cosine similarity are shown in Table 6.

Again, the overall best results are achieved with SFace features, which are partly better than when using cosine similarity. However, the average performance across all face descriptors assessed is slightly lower. Another noticeable difference is that the  $\theta$  and  $\lambda$  values with which the best results are achieved are significantly higher. The mean and standard deviation of the genuine and imposter score distributions in terms of the Euclidean distance is shown in Table 7. It can be seen that they are clearly higher than in Table 4 (cosine similarity). The IoUs, however, are identical. The identical IoUs could be due to the fact that the features are normalized before calculating the Euclidean distance. Thus, when using the Euclidean distance, the scores are more or less scaled differently. For the differently scaled scores, better performance can also be achieved with Dlib features using a combination of biometric and appearance features (i.e.  $\lambda = 0.6$ ).

#### 4.4.7 Compare Tracker

In table 8 FaceSORT is compared with different state-of-the-art multi-face trackers. A comparison with StrongSORT including MC (i.e., when  $\lambda$  is equal 1.0 or 0.0) is already performed in ‘1) Selection of a fixed  $\lambda$ ’. The FaceSORT results are obtained with SFace features,  $\lambda = 0.1$  and  $\theta = 0.2$ . Implementations are available for the MCFDR<sup>7</sup> and UMA<sup>8</sup>. However, no implementation is available for the OMTMCM multi-face tracker. For this reason, OMTMCM is carefully implemented according to the description in [42]. To verify the implementation, the results for the MusicVideo dataset [70] are also presented in table 8. The MusicVideo dataset consists of 8 music videos (i.e., Apink, BrunoMars, Darling, GirlsAloud, HelloBubble, PussycatDolls, Tara and Westlife) from YouTube, is publicly available<sup>9</sup> and was used in [42] to evaluate the proposed OMTMCM multi-face tracker. Since music videos are unconstrained videos (with different scenes,

<sup>7</sup><https://github.com/yjwong1999/OpenVINO-Face-Tracking-using-YOLOv8-and-DeepSORT>

<sup>8</sup><https://github.com/yinjunbo/UMA-MOT>

<sup>9</sup><https://sites.google.com/site/shunzhang876/eccv16-face-tracking>

Table 6: L2: Best achieved AssA, IDF1 and IDSW for different selections of  $\theta$  and  $\lambda$  combinations. Face descriptors: (1) ArcFace, (2) DeepFace, (3) DeepID, (4) Dlib, (5) Facenet, (6) Facenet512, (7) OpenFace, (8) SFace, (9) SeNet50, (10) VGG-Face and (11) ArcFaceII.

	PLUSFiaQ						ChokePoint					
	$\theta/\lambda$	AssA $\uparrow$	$\theta/\lambda$	IDF1 $\uparrow$	$\theta/\lambda$	IDSW $\downarrow$	$\theta/\lambda$	AssA $\uparrow$	$\theta/\lambda$	IDF1 $\uparrow$	$\theta/\lambda$	IDSW $\downarrow$
(1)	0.55/0.1	0.6287	0.55/0.1	0.7325	0.85/0.1	0.0080	0.55/0.3	0.8365	0.55/0.3	0.8801	1.15/0.3	0.0051
(2)	0.6/0.4	0.6398	0.6/0.4	0.7375	0.8/0.1	0.0080	0.7/0.6	0.8410	0.7/0.5	0.8839	0.9/0.9	0.0054
(3)	0.49/0.1	0.6215	0.49/0.1	0.7264	0.56/0.1	0.0086	0.6/0.4	0.8371	0.6/0.4	0.8803	0.8/0.8	0.0057
(4)	0.4/0.6	0.6444	0.4/0.6	0.7338	0.56/0.0	0.0091	0.4/0.6	0.8399	0.4/0.6	0.8793	0.4/0.8	0.0078
(5)	0.55/0.1	0.6395	0.55/0.1	0.7389	0.85/0.2	0.0080	0.55/0.3	0.8310	0.55/0.3	0.8723	1.15/0.4	0.0051
(6)	<b>0.7/0.4</b>	<b>0.6762</b>	0.7/0.4	0.7560	0.85/0.3	0.0079	0.85/0.5	0.8539	0.85/0.5	0.8882	1.15/0.4	0.0051
(7)	0.6/0.4	0.6398	0.7/0.6	0.7382	0.8/0.2	0.0080	0.6/0.3	0.8272	0.6/0.3	0.8731	0.9/0.6	0.0055
(8)	0.85/0.4	0.6672	<b>0.85/0.4</b>	<b>0.7636</b>	<b>1.15/0.7</b>	<b>0.0074</b>	<b>1.15/0.9</b>	<b>0.8800</b>	<b>1.0/0.6</b>	<b>0.9010</b>	<b>1.3/0.3</b>	<b>0.0047</b>
(9)	0.49/0.3	0.6376	0.49/0.3	0.7353	0.56/0.4	0.0081	0.6/0.4	0.8409	0.6/0.4	0.8781	0.8/0.6	0.0050
(10)	0.7/0.4	0.6565	0.7/0.4	0.7469	0.85/0.1	0.0079	0.7/0.6	0.8562	0.85/0.6	0.8872	1.15/0.9	0.0051
(11)	0.7/0.3	0.6613	0.7/0.3	0.7520	1.0/0.6	0.0077	1.0/0.8	0.8574	1.0/0.8	0.8925	1.0/0.7	0.0051
$\emptyset$	0.60/0.32	0.6466	0.61/0.34	0.7419	0.80/0.25	0.0081	0.70/0.52	0.8455	0.70/0.48	0.8833	0.97/0.61	0.0054

Table 7: L2: Presents the overlap (IoU) between the genuine and imposter scores as well as their mean ( $\mu$ ) and standard deviation ( $\sigma$ ). Feature models: (1) ArcFace, (2) DeepFace, (3) DeepID, (4) Dlib, (5) Facenet, (6) Facenet512, (7) OpenFace, (8) SFace, (9) SeNet50, (10) VGG-Face, (11) ArcFaceII and (12) Appearance Features.

	PLUSFiaQ			ChokePoint		
	IoU	genuine $\mu/\sigma$	imposter $\mu/\sigma$	IoU	genuine $\mu/\sigma$	imposter $\mu/\sigma$
(1)	0.26	0.45/0.26	0.95/0.37	0.20	0.48/0.27	1.01/0.35
(2)	0.14	0.41/0.15	0.70/0.11	0.12	0.43/0.15	0.72/0.11
(3)	0.20	0.18/0.12	0.41/0.14	0.17	0.20/0.13	0.43/0.13
(4)	0.07	0.19/0.06	0.37/0.06	0.08	0.21/0.06	0.38/0.07
(5)	0.18	0.43/0.22	0.97/0.28	0.26	0.44/0.25	0.90/0.32
(6)	0.07	0.52/0.23	1.22/0.17	0.09	0.57/0.23	1.19/0.20
(7)	0.18	0.43/0.16	0.77/0.17	0.18	0.45/0.16	0.81/0.20
(8)	<b>0.04</b>	0.71/0.22	1.31/0.10	<b>0.04</b>	0.74/0.20	1.34/0.09
(9)	0.18	0.19/0.10	0.41/0.13	0.19	0.28/0.15	0.67/0.23
(10)	0.07	0.52/0.19	1.09/0.14	0.08	0.60/0.18	1.14/0.17
(11)	0.08	0.61/0.22	1.23/0.15	0.05	0.65/0.19	1.27/0.13
(12)	0.16	0.20/0.11	0.70/0.29	0.18	0.23/0.13	0.67/0.28

moving camera, etc.), they do not correspond to the considered scenario in which people move towards a gate for which FaceSORT is designed. For this dataset, OMTMCM performed best. However, in the considered scenario where people are moving towards a gate (PLUSFiaQ and ChokePoint), FaceSORT clearly outperformed the other evaluated state-of-the-art trackers.

## 5 Ablation Study

The main components of FaceSORT are the combination of biometric and appearance features, the matching cascade and IoU fallback matching. Running FaceSORT with either biometric (i.e.,  $\lambda = 1.0$ ) or appearance features (i.e.,  $\lambda = 0.0$ ) has already been evaluated in ‘1) Selection of a fixed  $\lambda$ ’ of subsection 4.4.

In the matching cascade (described in section 2), the tracks that were successfully matched in the previous frame are considered first. This can reduce the search space  $\Phi$  and can be particularly beneficial if long occlusions are allowed (i.e., a

large active track memory  $\Phi$ ). For all experiments, occlusions up to 100 frames are allowed (i.e.,  $N_{max} = 100$ ). In table 9, execution times in frames per second (fps) are reported for FaceSORT with and without the matching cascade (MC) and compared with the re-implementation of a state-of-the-art tracker (i.e., OMTMCM [42]). All times were recorded on a standard desktop PC (i.e., Intel Core i5 gen9) and without taking face detection and feature extraction into account. It can be seen that the fps increases slightly when MC is applied. This is also reflected by the observation that on average less than half of all stored active tracks are required to successfully match all detected faces. However, applying the MC carries the risk that not the best matches are found. For example, it could happen that the best match (lowest cost) for a detected face is with a track that could not be matched in the last frames (e.g., a person returning from an occlusion), but the detected face is matched with a track that is tried in the MC before. The achieved tracking performance scores for FaceSORT (with SFace features,  $\lambda = 0.1$  and  $\theta = 0.2$ ) without the matching cascade (MC) are reported in table 8. Compared to results when using the matching cascade (table 8 first row) a performance decrease can be observed.

IoU fallback matching is applied to all unmatched detections after the matching cascade, including matching with tentative tracks (only confirmed tracks are considered in the matching cascade). To achieve the reported tracking performance of FaceSORT (table 8 first row), IoU matching is performed for 3.91%, 4.9% and 8.42% of all detected faces of the PLUSFiaQ, ChokePoint and MusicVideo dataset respectively. When disabling IoU fallback matching (IoU) the performance decreases significantly (see table 8). The performance achieved when FaceSORT is applied without matching cascade and IoU fallback matching is reported in table 8 (last row).

## 6 Conclusion

It this work, a new multi-face tracking method, FaceSORT, is proposed. To mitigate the problem of partially occluded and

Table 8: Compare FaceSORT with state-of-the-art multi-face tracker, where **MC** and **IoU** denote FaceSORT without matching cascade (MC) and/or IoU fallback matching.

	PLUSFiaQ					ChokePoint					MusicVideo			
	AssA $\uparrow$	HOTA $\uparrow$	IDF1 $\uparrow$	IDSW $\downarrow$		AssA $\uparrow$	HOTA $\uparrow$	IDF1 $\uparrow$	IDSW $\downarrow$		AssA $\uparrow$	HOTA $\uparrow$	IDF1 $\uparrow$	IDSW $\downarrow$
FaceSORT	<b>0.6527</b>	<b>0.7486</b>	<b>0.7338</b>	0.0104	<b>0.8404</b>	<b>0.8672</b>	<b>0.8783</b>	0.0081	0.0425	0.1821	0.0918	0.0343		
OMTMCM[42]	0.2039	0.3765	0.3352	0.1671	0.2430	0.4483	0.4140	0.1335	<b>0.1077</b>	<b>0.2842</b>	<b>0.2383</b>	0.0944		
MCFDR[36]	0.4770	0.5886	0.0740	<b>0.0097</b>	0.5514	0.5432	0.0144	<b>0.0014</b>	0.0274	0.1142	0.0063	<b>0.0053</b>		
UMA[18]	0.1854	0.2531	0.2640	0.0437	0.5483	0.6932	0.6788	0.0112	0.0490	0.1933	0.0988	0.0268		
FaceSORT <b>MC</b>	0.5940	0.7147	0.7025	0.0169	0.8274	0.8603	0.8700	0.0107	0.0405	0.1776	0.0875	0.0400		
FaceSORT <b>IoU</b>	0.5764	0.7033	0.6760	0.0187	0.6933	0.7863	0.7671	0.0283	0.0363	0.1676	0.0830	0.0494		
FaceSORT <b>MC IoU</b>	0.5589	0.6924	0.6666	0.0292	0.6697	0.7721	0.7521	0.0392	0.0359	0.1664	0.0812	0.0618		

Table 9: Frames per second for FaceSORT (FS), FaceSORT without the matching cascade (FS **MC**) and OMTMCM [42].

PLUSFiaQ			ChokePoint		
FS	FS <b>MC</b>	OMTMCM	FS	FS <b>MC</b>	OMTMCM
90.43	87.25	71.14	143.03	134.99	134.01

lateral faces, two different features (i.e., face (biometric) and appearance features) are combined. In the considered scenario, when people move towards a gate/portal (PLUSFiaQ and ChokePoint dataset) FaceSORT clearly outperformed the evaluated state-of-the-art tracker. To get a deeper insight into the proposed method, a comprehensive experimental evaluation and an ablation study are conducted. It is shown that the selection of the face descriptor and the similarity measure, as well as the resulting distribution of genuine and imposter scores are crucial. In general, selecting a low similarity threshold  $\theta$  and a high parameter  $\lambda$  lead to a high AssPr.

For future work, an adaptive  $\lambda$  could be evaluated based on the detected faces, i.e. in crowded scenes with probably more partially occluded and lateral faces,  $\lambda$  could automatically decrease. Furthermore, the general similarity threshold  $\theta$  could be split into two thresholds, one for biometric and one for appearance features, to better account for the different distributions of imposter and genuine scores. A different idea would be to perform association based on biometric features first and apply appearance based association as fallback.

## References

- [1] W. Luo, J. Xing, A. Milan, X. Zhang, W. Liu, T.-K. Kim, Multiple object tracking: A literature review, *Artificial Intelligence* 293 (2021) 103448. doi:10.1016/j.artint.2020.103448.
- [2] T. Meinhardt, A. Kirillov, L. Leal-Taixe, C. Feichtenhofer, Trackformer: Multi-object tracking with transformers, in: *Proceedings of the IEEE/CVF conference on computer vision and pattern recognition, 2022*, pp. 8844–8854.
- [3] K. Deng, C. Zhang, Z. Chen, W. Hu, B. Li, F. Lu, Jointing recurrent across-channel and spatial attention for multi-object tracking with block-erasing data augmentation, *IEEE Transactions on Circuits and Systems for Video Technology* 33 (8) (2023) 4054–4069. doi:10.1109/TCSVT.2023.3238716.
- [4] Y. Jin, F. Gao, J. Yu, J. Wang, F. Shuang, Multi-object tracking: Decoupling features to solve the contradictory dilemma of feature requirements, *IEEE Transactions on Circuits and Systems for Video Technology* 33 (9) (2023) 5117–5132. doi:10.1109/TCSVT.2023.3249162.
- [5] D. Chen, H. Shen, Y. Shen, Jdt-nas: Designing efficient multi-object tracking architectures for non-gpu computers, *IEEE Transactions on Circuits and Systems for Video Technology* 33 (12) (2023) 7541–7553. doi:10.1109/TCSVT.2023.3275813.
- [6] W. Lv, N. Zhang, J. Zhang, D. Zeng, One-shot multiple object tracking with robust id preservation, *IEEE Transactions on Circuits and Systems for Video Technology* 34 (6) (2024) 4473–4488. doi:10.1109/TCSVT.2023.3339609.
- [7] Z. Sun, J. Chen, L. Chao, W. Ruan, M. Mukherjee, A survey of multiple pedestrian tracking based on tracking-by-detection framework, *IEEE Transactions on Circuits and Systems for Video Technology* 31 (5) (2021) 1819–1833. doi:10.1109/TCSVT.2020.3009717.
- [8] H. Zhou, W. Ouyang, J. Cheng, X. Wang, H. Li, Deep continuous conditional random fields with asymmetric inter-object constraints for online multi-object tracking, *IEEE Transactions on Circuits and Systems for Video Technology* 29 (4) (2019) 1011–1022. doi:10.1109/TCSVT.2018.2825679.
- [9] H. Nodehi, A. Shahbahrami, Multi-metric re-identification for online multi-person tracking, *IEEE Transactions on Circuits and Systems for Video Technology* 32 (1) (2022) 147–159. doi:10.1109/TCSVT.2021.3059250.
- [10] S. You, H. Yao, C. Xu, Multi-object tracking with spatial-temporal topology-based detector, *IEEE Transactions on Circuits and Systems for Video Technology* 32 (5) (2022) 3023–3035. doi:10.1109/TCSVT.2021.3096237.

- [11] T.-Y. Chung, M. Cho, H. Lee, S. Lee, Ssat: Self-supervised associating network for multiobject tracking, *IEEE Transactions on Circuits and Systems for Video Technology* 32 (11) (2022) 7858–7868. doi:10.1109/TCSVT.2022.3186751.
- [12] M. Hu, X. Zhu, H. Wang, S. Cao, C. Liu, Q. Song, Std-former: Spatial-temporal motion transformer for multiple object tracking, *IEEE Transactions on Circuits and Systems for Video Technology* 33 (11) (2023) 6571–6594. doi:10.1109/TCSVT.2023.3263884.
- [13] K. Shim, J. Byun, K. Ko, J. Hwang, C. Kim, Enhancing robustness of multi-object trackers with temporal feature mix, *IEEE Transactions on Circuits and Systems for Video Technology* (2024) 1–1doi:10.1109/TCSVT.2024.3403166.
- [14] H. W. Kuhn, The hungarian method for the assignment problem, *Naval Research Logistics Quarterly* 2 (1-2) (1955) 83–97. arXiv:<https://onlinelibrary.wiley.com/doi/pdf/10.1002/nav.3800020109>, doi:10.1002/nav.3800020109. URL <https://onlinelibrary.wiley.com/doi/abs/10.1002/nav.3800020109>
- [15] A. Bewley, Z. Ge, L. Ott, F. Ramos, B. Upcroft, Simple online and realtime tracking, in: 2016 IEEE International Conference on Image Processing (ICIP), 2016, pp. 3464–3468. doi:10.1109/ICIP.2016.7533003.
- [16] N. Wojke, A. Bewley, D. Paulus, Simple online and realtime tracking with a deep association metric, in: 2017 IEEE International Conference on Image Processing (ICIP), 2017, p. 3645–3649. doi:10.1109/ICIP.2017.8296962.
- [17] Y. Du, Z. Zhao, Y. Song, Y. Zhao, F. Su, T. Gong, H. Meng, Strongsort: Make deepsort great again, *IEEE Transactions on Multimedia* 25 (2023) 8725–8737. doi:10.1109/TMM.2023.3240881.
- [18] J. Yin, W. Wang, Q. Meng, R. Yang, J. Shen, A unified object motion and affinity model for online multi-object tracking, in: Proceedings of the IEEE/CVF Conference on Computer Vision and Pattern Recognition, 2020, pp. 6768–6777.
- [19] J. Seidenschwarz, G. Brasó, V. C. Serrano, I. Elezi, L. Leal-Taixé, Simple cues lead to a strong multi-object tracker, in: Proceedings of the IEEE/CVF Conference on Computer Vision and Pattern Recognition (CVPR), 2023, p. 13813–13823.
- [20] H. Sheng, J. Chen, Y. Zhang, W. Ke, Z. Xiong, J. Yu, Iterative multiple hypothesis tracking with tracklet-level association, *IEEE Transactions on Circuits and Systems for Video Technology* 29 (12) (2019) 3660–3672. doi:10.1109/TCSVT.2018.2881123.
- [21] H. Sheng, Y. Zhang, J. Chen, Z. Xiong, J. Zhang, Heterogeneous association graph fusion for target association in multiple object tracking, *IEEE Transactions on Circuits and Systems for Video Technology* 29 (11) (2019) 3269–3280. doi:10.1109/TCSVT.2018.2882192.
- [22] J. Deng, J. Guo, N. Xue, S. Zafeiriou, Arcface: Additive angular margin loss for deep face recognition, in: 2019 IEEE/CVF Conference on Computer Vision and Pattern Recognition (CVPR), 2019, pp. 4685–4694. doi:10.1109/CVPR.2019.00482.
- [23] Y. Guo, L. Zhang, Y. Hu, X. He, J. Gao, Ms-celeb-1m: A dataset and benchmark for large-scale face recognition, in: Computer Vision–ECCV 2016: 14th European Conference, Amsterdam, The Netherlands, October 11–14, 2016, Proceedings, Part III 14, Springer, 2016, pp. 87–102.
- [24] Q. Zhao, S. Wang, Real-time face tracking in surveillance videos on chips for valuable face capturing, in: 2020 International Conference on Artificial Intelligence and Computer Engineering (ICAICE), 2020, pp. 281–284. doi:10.1109/ICAICE51518.2020.00060.
- [25] J. Wang, J. Lang, Visual multi-face tracking applied to council proceedings, *IEEE Instrumentation & Measurement Magazine* 24 (3) (2021) 78–84.
- [26] K. Zhang, Z. Zhang, Z. Li, Y. Qiao, Joint face detection and alignment using multitask cascaded convolutional networks, *IEEE Signal Processing Letters* 23 (10) (2016) 1499–1503. doi:10.1109/LSP.2016.2603342.
- [27] W. Liu, D. Anguelov, D. Erhan, C. Szegedy, S. Reed, C.-Y. Fu, A. C. Berg, Ssd: Single shot multibox detector, in: Computer Vision–ECCV 2016: 14th European Conference, Amsterdam, The Netherlands, October 11–14, 2016, Proceedings, Part I 14, Springer, 2016, pp. 21–37.
- [28] J. Dai, Y. Li, K. He, J. Sun, R-fcn: Object detection via region-based fully convolutional networks, *Advances in neural information processing systems* 29 (2016).
- [29] N. Wojke, A. Bewley, Deep cosine metric learning for person re-identification, in: 2018 IEEE Winter Conference on Applications of Computer Vision (WACV), 2018, pp. 748–756. doi:10.1109/WACV.2018.00087.
- [30] W. Liu, Y. Wen, Z. Yu, M. Li, B. Raj, L. Song, Sphreface: Deep hypersphere embedding for face recognition, in: Proceedings of the IEEE conference on computer vision and pattern recognition, 2017, pp. 212–220.
- [31] Y. Alayary, N. Shoukry, M. A. A. El Ghany, M. A.-M. Salem, Face masked and unmasked humans detection and tracking in video surveillance, in: 2022 4th

- Novel Intelligent and Leading Emerging Sciences Conference (NILES), 2022, pp. 211–215. doi:10.1109/NILES56402.2022.9942375.
- [32] T. M. Tran, N. H. Tran, S. T. M. Duong, H. D. Ta, C. D. Nguyen, T. Bui, S. Q. Truong, Resort: an id-recovery multi-face tracking method for surveillance cameras, in: 2021 16th IEEE International Conference on Automatic Face and Gesture Recognition (FG 2021), 2021, pp. 01–08. doi:10.1109/FG52635.2021.9666941.
- [33] D. Marčetić, S. Ribarić, An online multi-face tracker for unconstrained videos, in: 2018 14th International Conference on Signal-Image Technology & Internet-Based Systems (SITIS), 2018, pp. 159–165. doi:10.1109/SITIS.2018.00033.
- [34] G. Barquero, C. Fernández, I. Hupont, Long-term face tracking for crowded video-surveillance scenarios, in: 2020 IEEE International Joint Conference on Biometrics (IJCB), 2020, pp. 1–8. doi:10.1109/IJCB48548.2020.9304892.
- [35] F. Pernici, M. Bruni, A. Del Bimbo, Self-supervised online cumulative learning from video streams, *Computer Vision and Image Understanding* 197-198 (2020) 102983. doi:10.1016/j.cviu.2020.102983.
- [36] Y. J. Wong, K. Huang Lee, M.-L. Tham, B.-H. Kwan, Multi-camera face detection and recognition in unconstrained environment, in: 2023 IEEE World AI IoT Congress (AIIoT), 2023, pp. 0548–0553. doi:10.1109/AIIoT58121.2023.10174362.
- [37] J. Redmon, S. Divvala, R. Girshick, A. Farhadi, You only look once: Unified, real-time object detection, in: 2016 IEEE Conference on Computer Vision and Pattern Recognition (CVPR), 2016, pp. 779–788. doi:10.1109/CVPR.2016.91.
- [38] W. Liu, Y. Wen, B. Raj, R. Singh, A. Weller, Sphereface revived: Unifying hyperspherical face recognition, *IEEE Transactions on Pattern Analysis and Machine Intelligence* 45 (2) (2023) 2458–2474. doi:10.1109/TPAMI.2022.3159732.
- [39] O. Parkhi, A. Vedaldi, A. Zisserman, Deep face recognition, in: BMVC 2015-Proceedings of the British Machine Vision Conference 2015, British Machine Vision Association, 2015.
- [40] F. Schroff, D. Kalenichenko, J. Philbin, Facenet: A unified embedding for face recognition and clustering, in: Proceedings of the IEEE Conference on Computer Vision and Pattern Recognition (CVPR), 2015.
- [41] Y. Zhong, W. Deng, J. Hu, D. Zhao, X. Li, D. Wen, Sface: Sigmoid-constrained hypersphere loss for robust face recognition, *IEEE Transactions on Image Processing* 30 (2021) 2587–2598. doi:10.1109/TIP.2020.3048632.
- [42] Z. Weng, H. Zhuang, H. Li, B. Ramalingam, R. E. Mohan, Z. Lin, Online multi-face tracking with multimodality cascaded matching, *IEEE Transactions on Circuits and Systems for Video Technology* 33 (6) (2023) 2738–2752. doi:10.1109/TCSVT.2022.3224699.
- [43] J. Hu, L. Shen, G. Sun, Squeeze-and-excitation networks, in: Proceedings of the IEEE Conference on Computer Vision and Pattern Recognition (CVPR), 2018.
- [44] Q. Cao, L. Shen, W. Xie, O. M. Parkhi, A. Zisserman, Vggface2: A dataset for recognising faces across pose and age, in: 2018 13th IEEE International Conference on Automatic Face & Gesture Recognition (FG 2018), 2018, pp. 67–74. doi:10.1109/FG.2018.00020.
- [45] K. He, X. Zhang, S. Ren, J. Sun, Deep residual learning for image recognition, in: Proceedings of the IEEE Conference on Computer Vision and Pattern Recognition (CVPR), 2016.
- [46] Q. Huang, Y. Xiong, A. Rao, J. Wang, D. Lin, Movienet: A holistic dataset for movie understanding, in: Computer Vision—ECCV 2020: 16th European Conference, Glasgow, UK, August 23–28, 2020, Proceedings, Part IV 16, Springer, 2020, pp. 709–727.
- [47] Y. Wong, S. Chen, S. Mau, C. Sanderson, B. C. Lovell, Patch-based probabilistic image quality assessment for face selection and improved video-based face recognition, in: IEEE Biometrics Workshop, Computer Vision and Pattern Recognition (CVPR) Workshops, IEEE, 2011, pp. 81–88.
- [48] Z. Wang, L. Zheng, Y. Liu, Y. Li, S. Wang, Towards real-time multi-object tracking, in: European conference on computer vision, Springer, 2020, pp. 107–122.
- [49] Y. Du, J. Wan, Y. Zhao, B. Zhang, Z. Tong, J. Dong, Giauotracker: A comprehensive framework for mcmot with global information and optimizing strategies in visdrone 2021, in: Proceedings of the IEEE/CVF International Conference on Computer Vision (ICCV) Workshops, 2021, pp. 2809–2819.
- [50] A. Dutta, A. Zisserman, The VIA annotation software for images, audio and video, in: Proceedings of the 27th ACM International Conference on Multimedia, MM '19, ACM, New York, NY, USA, 2019. doi:10.1145/3343031.3350535. URL <https://doi.org/10.1145/3343031.3350535>
- [51] P. Dendorfer, H. Rezatofighi, A. Milan, J. Shi, D. Cremers, I. Reid, S. Roth, K. Schindler, L. Leal-Taixé,



- Mot20: A benchmark for multi object tracking in crowded scenes, arXiv:2003.09003[cs]ArXiv: 2003.09003 (Mar. 2020).  
URL <http://arxiv.org/abs/1906.04567>
- [52] J. Deng, W. Dong, R. Socher, L.-J. Li, K. Li, L. Fei-Fei, Imagenet: A large-scale hierarchical image database, in: 2009 IEEE conference on computer vision and pattern recognition, Ieee, 2009, pp. 248–255.
- [53] S. I. Serengil, A. Ozpinar, Lightface: A hybrid deep face recognition framework, in: 2020 Innovations in Intelligent Systems and Applications Conference (ASYU), IEEE, 2020, pp. 23–27. doi:10.1109/ASYU50717.2020.9259802.  
URL <https://doi.org/10.1109/ASYU50717.2020.9259802>
- [54] S. I. Serengil, A. Ozpinar, Hyperextended lightface: A facial attribute analysis framework, in: 2021 International Conference on Engineering and Emerging Technologies (ICEET), IEEE, 2021, pp. 1–4. doi:10.1109/ICEET53442.2021.9659697.  
URL <https://doi.org/10.1109/ICEET53442.2021.9659697>
- [55] G. B. Huang, M. Mattar, T. Berg, E. Learned-Miller, Labeled faces in the wild: A database for studying face recognition in unconstrained environments, in: Workshop on faces in 'Real-Life' Images: detection, alignment, and recognition, 2008.
- [56] L. Wolf, T. Hassner, I. Maoz, Face recognition in unconstrained videos with matched background similarity, in: CVPR 2011, IEEE, 2011, pp. 529–534.
- [57] D. Yi, Z. Lei, S. Liao, S. Z. Li, Learning face representation from scratch, arXiv preprint arXiv:1411.7923 (2014).
- [58] B. Amos, B. Ludwiczuk, M. Satyanarayanan, Openface: A general-purpose face recognition library with mobile applications, Tech. rep., CMU-CS-16-118, CMU School of Computer Science (2016).
- [59] H.-W. Ng, S. Winkler, A data-driven approach to cleaning large face datasets, in: 2014 IEEE international conference on image processing (ICIP), IEEE, 2014, pp. 343–347.
- [60] Y. Taigman, M. Yang, M. Ranzato, L. Wolf, Deepface: Closing the gap to human-level performance in face verification, in: Proceedings of the IEEE Conference on Computer Vision and Pattern Recognition (CVPR), 2014.
- [61] Y. Sun, X. Wang, X. Tang, Deep learning face representation from predicting 10,000 classes, in: Proceedings of the IEEE Conference on Computer Vision and Pattern Recognition (CVPR), 2014.
- [62] Leondgarse, Keras insightface, [https://github.com/leondgarse/Keras\\_insightface](https://github.com/leondgarse/Keras_insightface) (2022). doi:10.5281/zenodo.6506949.
- [63] Davisking, Dlib, <https://github.com/davisking/dlib> (2022).
- [64] K. Bernardin, R. Stiefelhagen, Evaluating multiple object tracking performance: the clear mot metrics, EURASIP Journal on Image and Video Processing 2008 (2008) 1–10.
- [65] E. Ristani, F. Solera, R. Zou, R. Cucchiara, C. Tomasi, Performance measures and a data set for multi-target, multi-camera tracking, in: European conference on computer vision, Springer, 2016, pp. 17–35.
- [66] J. Luiten, A. Osep, P. Dendorfer, P. Torr, A. Geiger, L. Leal-Taixé, B. Leibe, Hota: A higher order metric for evaluating multi-object tracking, International journal of computer vision 129 (2) (2021) 548–578. doi:10.1007/s11263-020-01375-2.
- [67] F. Boutros, M. Fang, M. Klemm, B. Fu, N. Damer, Crifqa: Face image quality assessment by learning sample relative classifiability, in: Proceedings of the IEEE/CVF Conference on Computer Vision and Pattern Recognition (CVPR), 2023, pp. 5836–5845.
- [68] Q. Meng, S. Zhao, Z. Huang, F. Zhou, Magface: A universal representation for face recognition and quality assessment, in: Proceedings of the IEEE/CVF Conference on Computer Vision and Pattern Recognition (CVPR), 2021, pp. 14225–14234.
- [69] J. Hernandez-Ortega, J. Fierrez, I. Serna, A. Morales, Faceqgen: Semi-supervised deep learning for face image quality assessment, in: 2021 16th IEEE International Conference on Automatic Face and Gesture Recognition (FG 2021), 2021, pp. 1–8. doi:10.1109/FG52635.2021.9667060.
- [70] S. Zhang, Y. Gong, J.-B. Huang, J. Lim, J. Wang, N. Ahuja, M.-H. Yang, Tracking persons-of-interest via adaptive discriminative features, in: European Conference on Computer Vision, 2016, pp. 415–433.